Stochastic Seismic Response of Hysteretic Structures

AUTHOR(S):

KOBORI, Takuji; MINAI, Ryoichiro; SUZUKI, Yoshiyuki

CITATION:

KOBORI, Takuji ...[et al]. Stochastic Seismic Response of Hysteretic Structures. Bulletin of the Disaster Prevention Research Institute 1976, 26(1): 57-70

ISSUE DATE:

1976-03

URL:

http://hdl.handle.net/2433/124855

Bull. Disas. Prev. Res. Inst., Kyoto Univ., Vol. 26, Part 1, No. 236, March, 1976

Stochastic Seismic Response of Hysteretic Structures

Takuji KOBORI, Ryoichiro MINAI and Yoshiyuki SUZUKI

(Manuscript received March 22, 1976)

Abstract

An analytical procedure for the stochastic response analysis of hysteretic structures with strong nonlinearity to earthquake excitations is presented. For hysteretic nonlinear systems, statistical properties such as moments and probability densities of the responses cannot usually be obtained exactly. The present method is approximate but the solution is obtained without recourse to the equivalent linearization technique. The hysteretic characteristics such as bilinear and trilinear types are expressed in appropriate first-order differential forms with quasi-linear characteristics. These expressions give physical interpretation of hysteretic characteristics and make it possible to formulate the Fokker-Planck equation. The time-dependent statistics are then obtained as the solutions to a set of nonlinear first-order differential equations derived from the Fokker-Planck equation. As an illustration of the method, it is used to determine the response of a bilinear hysteretic system to a class of nonstationary excitations. Comparison of the results obtained here with those obtained by the simulation technique indicates that the proposed method is efficient for a stochastic seismic analysis of hysteretic systems, particularly for those with strong nonlinearity.

1. Introduction

Most building structures are designed to survive nonstationary random excitations such as earthquakes. Because of the severity of such excitations, the probabilistic determination of the seismic response of hysteretic systems with strong nonlinearity is of considerable practical importance in relation to the assessment of the ultimate anti-seismic structural safety. It seems that the Fokker-Planck equation approach[1] may be the only available method of obtaining the solution to this problem. Unfortunately, the exact solution to this equation has not yet been found. Therefore, several approximate approaches have been devised[2~7]. For hysteretic systems with strong nonlinearity, however, many of them are not adequate for application because of plastic drift, in other words, the fluctuation of the center of hysteresis due to strong softening effect[4]. Kaul and Penzien[5] have recently studied the transient response of bilinear hysteretic systems by using the Fokker-Planck equation approach combined with the equivalent linearization technique. However, as far as the equivalent linearization is used, some difficulties will arise in dealing with strong nonlinear systems having broad band frequency characteristics.

The purpose of this study is to present an approximate method of obtaining the nonstationary random response of hysteretic systems without recourse to the equivalent linearization technique. It is supposed that the excitation is either stationary or nonstationary Gaussian white noise with zero mean and that the system has polylinear hysteretic restoring force such as bilinear and trilinear types. It is shown that the

piecewise hysteretic characteristics can be expressed in the form of appropriate first-order quasi-linear differential equations, which make the Fokker-Planck formulation possible. The corresponding Fokker-Planck equation for such systems with hysteretic characteristics has multi-dimensional space greater than two-dimensions even for the second-order system with one degree-of-freedom. Under a certain simplified assumption with respect to the joint probability density of responses, a set of nonlinear first-order ordinary differential equations for moments or quasi-moments is derived from the Fokker-Planck equation. To confirm the validity of the method, numerical results of the present method are compared with those obtained through the Monte Carlo simulation technique.

2. Hysteretic System

In many studies on the dynamic response of structures, their yielding properties have been modeled by hysteretic restoring force characteristics, which depend on the past time history of the structural response. The hysteretic system considered here is mainly of the well-known bilinear hysteretic type. The bilinear hysteretic characteristic $\Phi(x,\dot{x})$ is chosen to have a unit rigidity for the first branch and a rigidity r for second branch, as shown in Fig. 1. Denoting the backlash characteristic by $\varphi(x,\dot{x})$ as shown in Fig. 2, the bilinear hysteretic characteristic $\Phi(x,\dot{x})$ can be written as

$$\Phi(x,\dot{x})=x-(1-r)\varphi(x,\dot{x}) \tag{1}$$

where x is the displacement nondimensionalized with reference to the elastic limit deformation, and the symbol $\cdot$ means the derivative with respect to time t. Introducing the new variable z defined on the range $[-1, 1]$, the backlash characteristic φ and its time derivative $\dot{\varphi}$ can be expressed in the following quasi-linear forms:

$$\varphi=x-z \qquad \text{where } |z| \leqq 1 \tag{2}$$

and

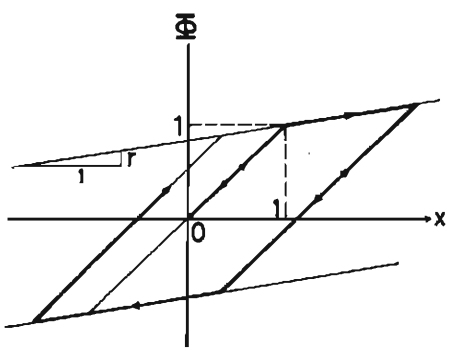

Fig. 1. Bilinear hysteretic characteristic.

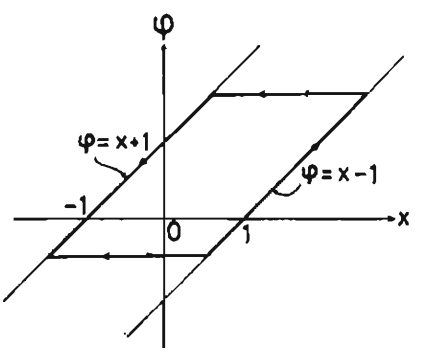

Fig. 2. Backlash characteristic.

$$\dot{\varphi}=g(\dot{x},z)=\begin{cases}\dot{x}U(\dot{x}) & ;\ z=1\\ 0 & ;\ |z|<1\\ \dot{x}U(-\dot{x}) & ;\ z=-1\end{cases} \tag{3}$$

where $U(\cdot)$ is the Heaviside unit step function. Equation (3) can be rewritten with respect to the variable z

$$\dot{z}=\dot{x}-g(\dot{x},z) \tag{4}$$

Furthermore, the above expressions can be easily extended to the polylinear hysteretic characteristics as follows:

$$\Phi(x,\dot{x})=x-\sum_{j=1}^{J}(r_j-r_{j+1})\varphi_j(x,\dot{x}) \tag{5}$$

and

$$\varphi_j=x-z_j \quad \text{where } |z_j|\leqq\delta_j \tag{6}$$

In the above equations, both r_1 and δ_1 are chosen to be unity, r_j is the rigidity of the j-th branch, δ_j is the deformation at the end of the j-th branch in the virgin curve, and φ_j has a backlash angle $2\delta_j$ and a unit slope. It is noted that $\Phi(x, \dot{x})$ becomes the bilinear and trilinear hysteresis when $J=1$ and $J=2$, respectively. The above-mentioned decomposition of the hysteretic characteristics can be interpreted according to the parallel-series model consisting of linear springs and Coulomb sliders as shown in Fig. 3[8]. In this model, φ_j corresponds to the plastic deformation of each slider, while z_j represents the deformation of each spring, in series to the slider, specified by the critical slipping force of the slip element δ_j.

The present expressions of hysteretic characteristics in the differential forms as given by Eqs. (3) and (4) are of great advantage in applying the Fokker-Planck equation approach, as will be illustrated in the following chapter.

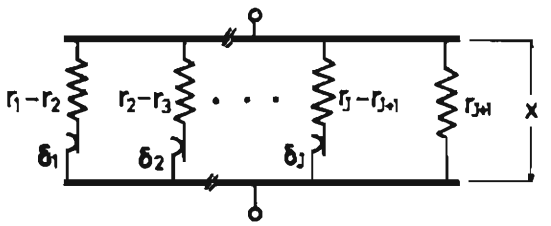

Fig. 3. Physical idealization of polylinear hysteretic characteristic.

3. Method of Solution

The dimensionless equation of motion of a single-degree-of-freedom bilinear hysteretic system is expressed as

$$\ddot{x}+2h\dot{x}+\Phi(x,\dot{x})=-f(t) \tag{7}$$

where h is the critical damping ratio. Here, the nondimensional displacement x,

time t and excitation $f(t)$ are respectively defined by

$$x=\frac{X}{\Delta},\quad t=\Omega_0 T \text{ and } f(t)=\frac{F(T)}{\Omega_0^2\Delta} \tag{8}$$

where X is the relative displacement, Δ is the elastic limit deformation, Ω_0 is the natural frequency of the associated linear system, T is time and $F(T)$ is the acceleration excitation. For the present study, the excitation $f(t)$ is a nonstationary Gaussian white noise defined by

$$f(t)=\alpha(t)\xi(t),\qquad \max_t |\alpha(t)|=1 \tag{9}$$

where $\alpha(t)$ represents an arbitrary deterministic envelope function, and $\xi(t)$ is the white noise with zero mean and uniform spectral density S_0, i.e.,

$$E[\xi(t)]=0,\qquad E[\xi(t)\,\xi(t+\tau)]=2\pi S_0\delta(\tau) \tag{10}$$

in which the symbol E denotes the ensemble average and $\delta(\cdot)$ is the Dirac delta function. Let $p(x, y, z; t)$ be the joint probability density function of the displacement x, the velocity $y(=\dot{x})$ and the extra state variable z under the condition that their initial values are zero at time $t=0$. The Fokker-Planck equation for $p(x, y, z; t)$ can be expressed as

$$\frac{\partial p}{\partial t}=-y\frac{\partial p}{\partial x}+\frac{\partial}{\partial y}\{[2hy+rx+(1-r)z]p\}+\frac{\partial}{\partial z}\{[g(y,z)-y]p\}+\frac{S(t)}{2}\frac{\partial^2 p}{\partial y^2} \tag{11}$$

where

$$S(t)=2\pi S_0\alpha^2(t) \tag{12}$$

No exact solution to Eq. (11) has been obtained to date.

Under the circumstances, a knowledge of the time-dependent moments of responses would be useful. The moments of responses are defined by

$$M(l,m,n;t)=E[x^l y^m z^n]=\int_{-\infty}^{\infty}\!\!\int\!\!\int x^l y^m z^n p(x,y,z;t)\,dx\,dy\,dz \tag{13}$$

where l, m, n are non-negative integers. It is shown that an infinite set of the following first-order differential equations can be derived from Eq. (11)

$$\begin{aligned}\dot{M}(l,m,n;t)=&lM(l-1,m+1,n;t)-m\{2hM(l,m,n;t)+rM(l+1,m-1,n;t)\\&+(1-r)M(l,m-1,n+1;t)\}+\frac{S(t)}{2}m(m-1)M(l,m-2,n;t)\\&+n\{M(l,m+1,n-1;t)-N(l,m,n;t)\}\end{aligned} \tag{14}$$

with the intial conditions

$$M(l,m,n;0)=0,\qquad N(l,m,n;0)=0 \tag{15}$$

where

$$M(0,0,0;t)=1 \tag{16}$$

$$N(l,m,n;t)=E[x^l y^m z^{n-1} g(y,z)]$$
$$=\int_{-\infty}^{\infty}\int\int x^l y^m z^{n-1} g(y,z)\, p(x,y,z;t)\,dx\,dy\,dz \tag{17}$$

Here, the unknown probability density function $p(x, y, z; t)$ in Eqs. (13) and (17) can be expressed in terms of quasi-moments B_{lmn}[9]

$$p(\boldsymbol{x};t)=w(\boldsymbol{x};t)\left[1+\sum_{s=3}^{\infty}\sum_{l+m+n=s}\frac{H_{lmn}(\boldsymbol{x})}{l!\,m!\,n!}\,B_{lmn}\right] \tag{18}$$

where $\boldsymbol{x}$ denotes the triplet (x, y, z), $w(\boldsymbol{x}; t)$ is the joint normal density function of the vector $\boldsymbol{x}$ and $H_{lmn}(\boldsymbol{x})$ are the three-dimensional Hermite polynomials, defined by

$$H_{lmn}(\boldsymbol{x})=(-1)^{l+m+n}e^{\frac{1}{2}\boldsymbol{x}^T\boldsymbol{K}^{-1}\boldsymbol{x}}\frac{\partial^{l+m+n}}{\partial x^l\partial y^m\partial z^n}e^{-\frac{1}{2}\boldsymbol{x}^T\boldsymbol{K}^{-1}\boldsymbol{x}} \tag{19}$$

In the above equation $\boldsymbol{K}$ is the covariance matrix of the vector $\boldsymbol{x}$. Furthermore, the cumulants C_{lmn} and quasi-moments B_{lmn} are mutually connected with the moments M_{lmn} by the relations

$$1+\sum_{s=1}^{\infty}\sum_{l+m+n=s}\frac{i^s}{l!\,m!\,n!}M_{lmn}\,u_1^l u_2^m u_3^n$$
$$=\exp\left[\sum_{s=1}^{\infty}\sum_{l+m+n=s}\frac{i^s}{l!\,m!\,n!}C_{lmn}\,u_1^l u_2^m u_3^n\right]$$
$$=e^{-\frac{1}{2}\boldsymbol{x}^T\boldsymbol{K}^{-1}\boldsymbol{x}}\left[1+\sum_{s=3}^{\infty}\sum_{l+m+n=s}\frac{i^s}{l!\,m!\,n!}B_{lmn}\,u_1^l u_2^m u_3^n\right] \tag{20}$$

where $\boldsymbol{u}$ is the triplet of the Fourier transformed parameters (u_1, u_2, u_3) corresponding to (x, y, z), and $i=\sqrt{-1}$. Using these relations, Eq. (14) can be replaced by the differential equations for the cumulants or quasi-moments.

According to the usual method of approximate analyses based on infinite series expressions, a "curtailment" of the system of differential equations is made such that quasi-moments higher than m-th order are neglected when quasi-moments up to the order m are concerned. The accuracy of the approximate solution depends on how satisfactorily the probability density $p(\boldsymbol{x}; t)$ is approximated by a curtailed series of Eq. (18). If the density function $p(\boldsymbol{x}; t)$ is close to Gaussian, the higher order quasi-moments are small, and it is possible to limit the analysis to a certain number of lower order quasi-moments.

In usual cases, attention is focused on the covariances of responses which are of primary interest. The responses of the hysteretic system are in general non-Gaussian random processes[3),4),6)]. In particular, it is evident from the difinition of z that the probability density function of z is quite dissimilar to the normal density function, whereas the probability distributions of x and y are relatively close to the normal distribution[4)]. Although the higher order quasi-moments are in general to be taken

into account with regard to the probability density function, which is necessary in calculating Eqs. (13) and (17)[6], an approximate analysis may be effectively performed for the present cases by introducing a simplified probability density function derived from the normal probability density function. From the definition of z, the probability density function may be assumed to be given approximately by the "truncated" form

$$p(x,y,z;t)=[U(z+1)-U(z-1)]w(x,y,z;t)+\delta(z-1)W_1(x,y;t)+\delta(z+1)W_2(x,y;t) \tag{21}$$

where $w(x, y, z; t)$ represents the normal density function with the covariance matrix $\boldsymbol{k}$. From the normalization condition for the density function, $W_1(x, y; t)$ and $W_2(x, y; t)$ are expressed as

$$W_1(x,y;t)=\int_1^{\infty} w(x,y,z;t)dz$$

$$W_2(x,y;t)=\int_{-\infty}^{-1} w(x,y,z;t)dz \tag{22}$$

By making use of the approximate density function given by Eq. (21), the desired covariance matrix $\boldsymbol{K}$ is expressed in terms of $\boldsymbol{k}$ as follows:

$$K_{xx}=k_{xx}, \quad K_{yy}=k_{yy}, \quad K_{xy}=k_{xy}$$

$$K_{zz}=k_{zz}\left[erf(\lambda)-\frac{2}{\sqrt{\pi}}\lambda e^{-\lambda^2}\right]+erfc(\lambda)$$

$$K_{xz}=k_{xz}\,erf(\lambda), \quad K_{yz}=k_{yz}\,erf(\lambda) \tag{23}$$

where

$$\lambda=\frac{1}{\sqrt{2k_{zz}}}$$

$$erf(\lambda)=\frac{2}{\sqrt{\pi}}\int_0^{\lambda}e^{-v^2}dv, \quad erfc(\lambda)=1-erf(\lambda)$$

To transform the differential equations for $\boldsymbol{K}$ obtained from Eq. (14) to those for $\boldsymbol{k}$, the following relationships between $\dot{\boldsymbol{K}}$ and $\dot{\boldsymbol{k}}$ are used:

$$\dot{k}_{xx}=\dot{K}_{xx}, \quad \dot{k}_{yy}=\dot{K}_{yy}, \quad \dot{k}_{xy}=\dot{K}_{xy}$$

$$\dot{k}_{zz}=\frac{\dot{K}_{zz}}{erf(\lambda)-\frac{2}{\sqrt{\pi}}\lambda e^{-\lambda^2}}$$

$$\dot{k}_{xz}=\frac{1}{erf(\lambda)}\left[\dot{K}_{xz}+\frac{\lambda}{\sqrt{\pi}}e^{-\lambda^2}k_{xz}\frac{\dot{k}_{zz}}{k_{zz}}\right]$$

$$\dot{k}_{yz}=\frac{1}{erf(\lambda)}\left[\dot{K}_{yz}+\frac{\lambda}{\sqrt{\pi}}e^{-\lambda^2}k_{yz}\frac{\dot{k}_{zz}}{k_{zz}}\right] \tag{24}$$

Combining the above relations of Eqs. (23) and (24) with Eq. (14), the first-order nonlinear differential equations with respect to $\boldsymbol{k}$ are obtained as

$$\dot{k}_{xx}=2k_{xy}$$

$$\dot{k}_{yy}=-2[2hk_{yy}+rk_{xy}+(1-r)k_{yz}\,erf(\lambda)]+S(t)$$

$$\dot{k}_{xy}=k_{yy}-2hk_{xy}-rk_{xx}-(1-r)k_{xz}\,erf(\lambda)$$

$$\dot{k}_{zz}=\frac{2}{erf(\lambda)-\frac{2}{\sqrt{\pi}}\lambda e^{-\lambda^2}}\,[k_{yz}\,erf(\lambda)-N_{002}]$$

$$\dot{k}_{xz}=k_{yz}+\frac{1}{erf(\lambda)}\left[k_{xy}+\frac{\lambda}{\sqrt{\pi}}e^{-\lambda^2}k_{xz}\frac{\dot{k}_{zz}}{k_{zz}}-N_{101}\right]$$

$$\dot{k}_{yz}=-2hk_{yz}-rk_{xz}+\frac{1}{erf(\lambda)}\Big[k_{yy}$$

$$-(1-r)k_{zz}(erf(\lambda)-\frac{2}{\sqrt{\pi}}\lambda e^{-\lambda^2})-(1-r)\,erfc(\lambda)$$

$$+k_{yz}\frac{\lambda}{\sqrt{\pi}}e^{-\lambda^2}\frac{\dot{k}_{zz}}{k_{zz}}-N_{011}\Big] \tag{25}$$

In above equations, terms N_{lmn} are given by

$$N_{002}=\sqrt{\frac{k_{yy}}{2\pi}}\,erfc\left(\frac{1}{\mu}\sqrt{\frac{k_{yy}}{2}}\right)+\frac{\lambda}{\sqrt{\pi}}e^{-\lambda^2}k_{yz}\left[1+erf\left(\frac{\lambda}{\mu}k_{yz}\right)\right]$$

$$N_{101}=b\,k_{yy}+c\,k_{yz}$$

$$N_{011}=b\,k_{xy}+c\,k_{xz} \tag{26}$$

where

$$b=\frac{1}{2}erfc(\lambda)+\frac{1}{\sqrt{\pi}}\int_{\lambda}^{\infty}e^{-v^2}\,erf\left(\frac{v}{\mu}k_{yz}\right)dv$$

$$c=\frac{\mu}{\pi k_{zz}}\exp\left(-\frac{k_{yy}}{2\mu^2}\right)+\frac{\lambda}{\sqrt{\pi}}e^{-\lambda^2}\frac{k_{yz}}{k_{zz}}\left[1+erf\left(\frac{\lambda}{\mu}k_{yz}\right)\right]$$

$$\mu=\sqrt{k_{yy}k_{zz}-k_{yz}^2}$$

The resulting "curtailed" system of differential equations of Eq. (25) is solved by using a digital computer. It is noted that $\boldsymbol{K}$ is the covariance matrix of the responses x, y and z, whereas $\boldsymbol{k}$ is the covariance matrix determining the approximate probability density function of Eq. (21).

4. Numerical Results

To verify the results obtained by the present approximate analytical method, a numerical simulation based on the Monte Carlo technique has been carried out.

For each case, the sample size of the ensemble of the response time-histories was 400, from which response statistics of interest were determined. Numerical results obtained from the analytical and simulation methods were presented for both the response processes under the stationary and nonstationary Gaussian white noise

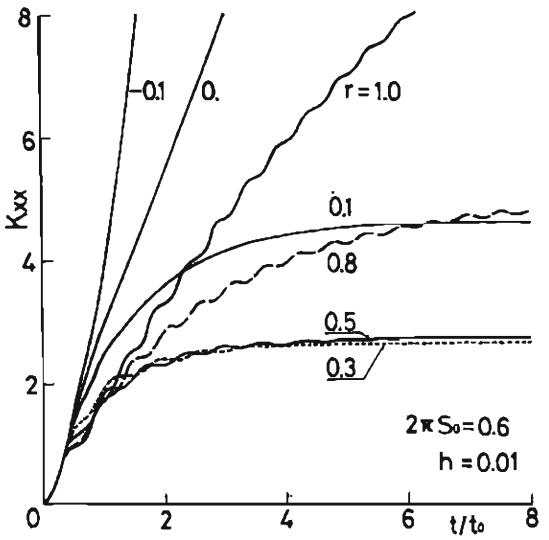

(a) Variance of displacement response

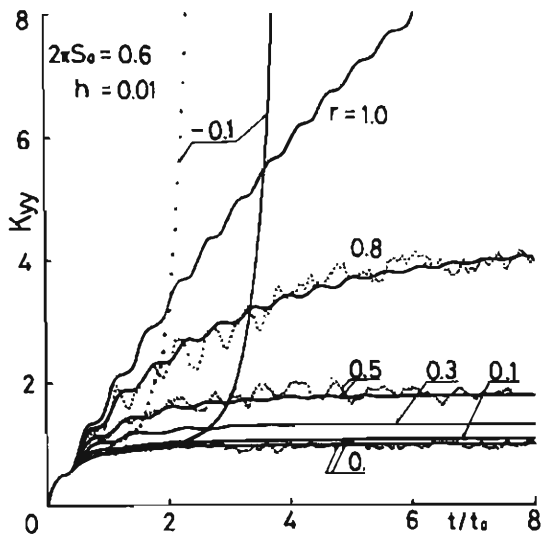

(b) Variance of velocity response

Fig. 4. Effect of the rigidity ratio r on the response to stationary excitation.
——, – – –, - - - : Theory ····· : Simulation

excitations.

Numerical results for the case of stationary excitation, i.e., $\alpha(t)=U(t)$, are shown in Figs. 4 through 6. Figures 4(a) and (b) give an indication of how the degree of nonlinearity represented by the rigidity ratio r affects the displacement and velocity

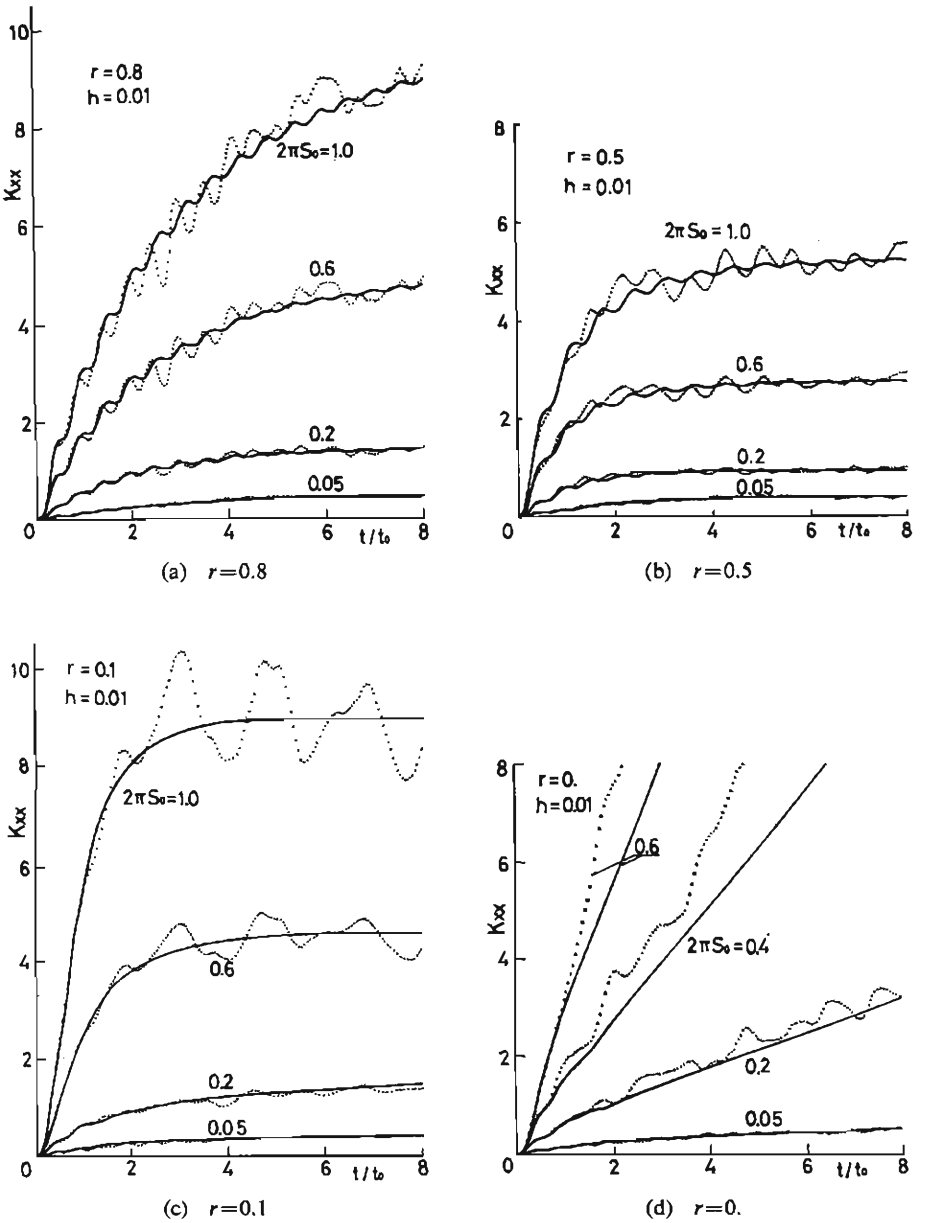

Fig. 5. Variance of displacement response to stationary excitations with various values of S_0.
—— : Theory ····· : Simulation

responses, respectively. The abscissas of these figures show the nondimensional time with reference to the natural period $t_0(=2\pi)$ of the associated linear system. In Fig. 5, the variance K_{xx} are shown for the various values of the level of the spectral density S_0 and the rigidity ratio r. Figure 6 shows the covariances K_{zz}, K_{xz} and K_{yz}. These figures also show the comparison of the analytical results with the simulated results. It is shown that the accuracy of the analytical method is satisfactory even for the cases of strong nonlinearity. Numerical results for the probability density function of the displacement response obtained from the simulation method are plotted in Fig. 7 along with the normal probability density function. From these results, the normal approximation for the probability density function of the displacement response appears to be reasonable for the cases that $r=0.5$ and 0.1, but it may not be a good approximation for the cases that $r\leqq 0$. In Fig. 8,

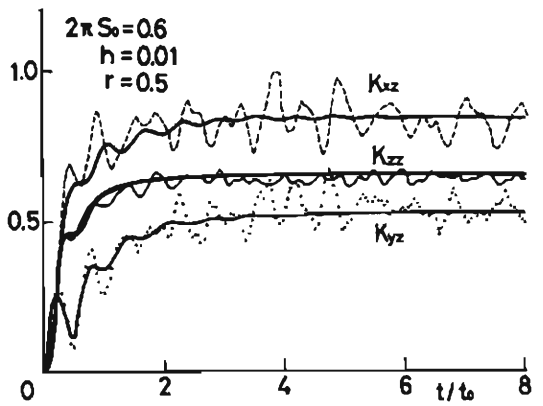

(a) $r=0.5$

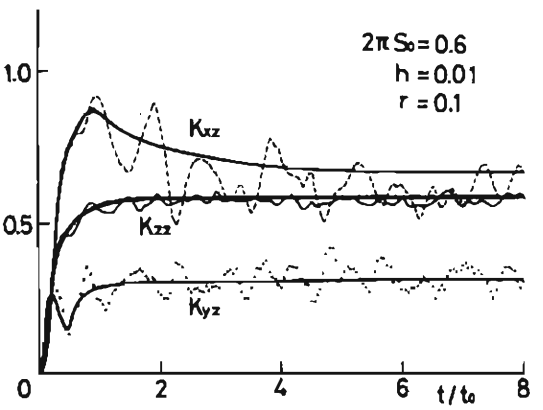

(b) $r=0.1$

Fig. 6. Covariances K_{zz}, K_{yz} and K_{xz} to stationary excitation.
——: Theory · · ·, ·····, ——: Simulation

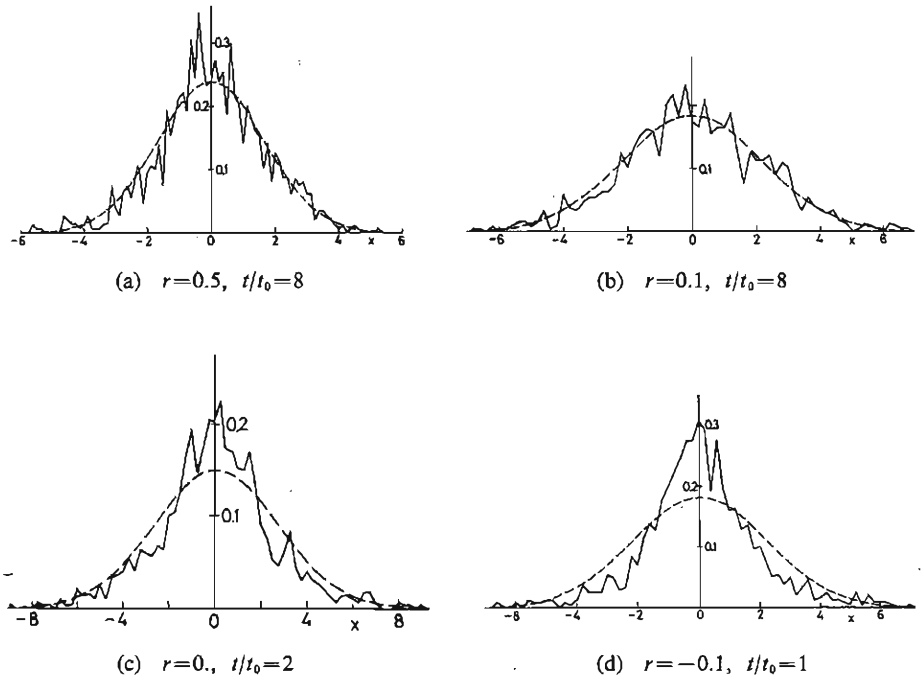

(a) $r=0.5,\ t/t_0=8$ (b) $r=0.1,\ t/t_0=8$

(c) $r=0.,\ t/t_0=2$ (d) $r=-0.1,\ t/t_0=1$

Fig. 7. Probability density function of the displacement response.
$2\pi S_0=0.6,\ h=0.01.$
——: Simulation (800 samples).
---: Normal probability density function.

three probability densities with respect to the extra state variable z are plotted: (i) the probability density obtained by the simulation, (ii) the normal density function with the variance K_{zz}, and (iii) the approximate probability density function derived from Eq. (21). It can be observed from Fig. 8 that the probability density function through the simulation is considerably different from the normal density function, and is relatively close to the approximate density function.

As an example of nonstationary excitation, an envelope function similar to that of earthquake excitations is considered. The envelope function shown in Fig. 9 is given by[10]

$$\alpha(t)=\beta t^{\frac{\gamma}{2}} e^{-\frac{\nu}{2}t} \tag{27}$$

wher $\beta=1.2698$, $\gamma=5.7076$ and $\nu=2.2830$. In Fig. 10, the results of the variances K_{xx} and K_{yy} are shown for various values of the rigidity ratio, and the validity of the present method is also demonstrated.

From the results of numerical examples, it is shown that the agreement between the results of the present analytical method and the those of simulation is satisfactory, except for the case of nonpositive rigidity ratio, i.e., $r\leqq 0$. The discrepancy between the two results for the case where $r\leqq 0$ may be due to the fact that the assumption of

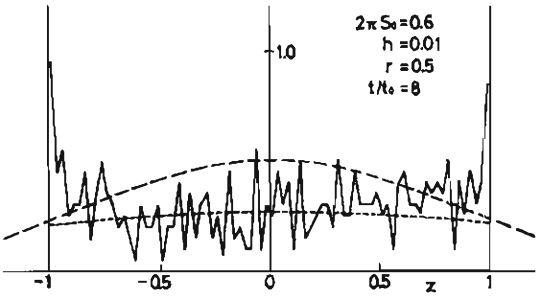

(a) $r=0.5$

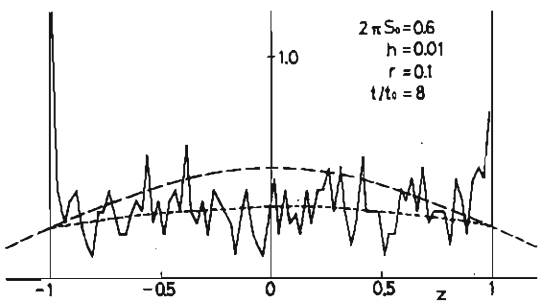

(b) $r=0.1$

Fig. 8. Probability density function of the extra state variable z.
– – – : Normal probability density function with variance K_{zz}.
····· : Approximate probability density function with variance k_{zz}.
—— : Simulation (800 samples).

the approximated probability density function given by Eq. (21) becomes invalid.

The general remark found from Figs. 4, 6 and 10 is that the response characteristics of the bilinear hysteretic systems are quite sensitive to the rigidity ratio. For any fixed value of the nondimensional excitation level S_0, the rigidity ratio which minimizes the displacement response is found to be in the range from 0.3 to 0.5. On the contrary, the velocity response decreases as the rigidity ratio becomes small except for $r<0$. For the case where $r<0$, both displacement and velocity responses increase rapidly within the short time-duration even for the nonstationary excitations considered here. It is suggested that such a large displacement response caused by the unstable increase of plastic drift might give rise to a serious problem on the seismic safety of hysteretic structures with the negative tangential rigidity in the plastic range[11].

5. Concluding Remarks

An analytical procedure to determine the stochastic response of hysteretic structures to earthquake-like excitations has been developed. The method is basically the

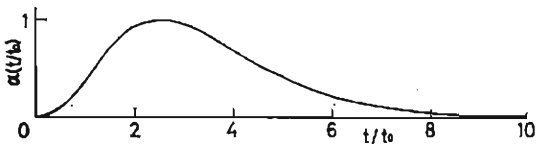

Fig. 9. Envelope function of nonstationary excitation.

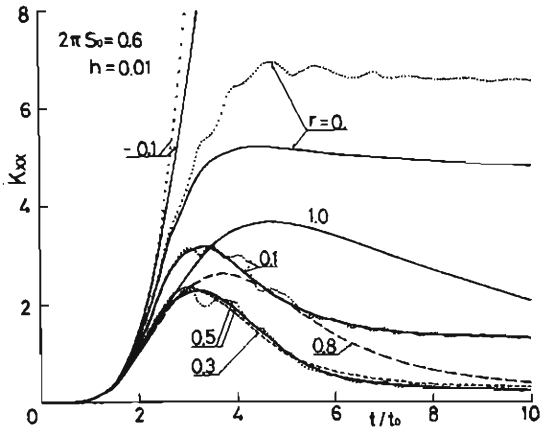

(a) Variance of displacement response

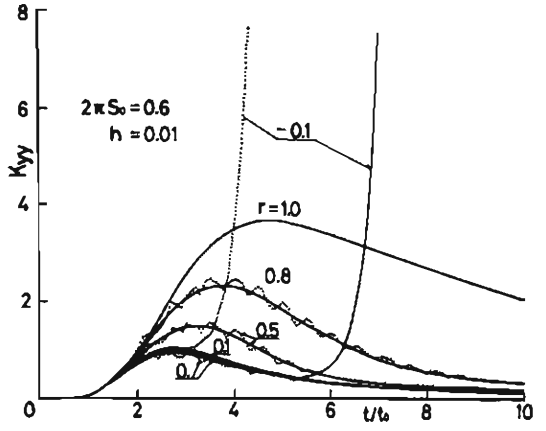

(b) Variance of velocity response

Fig. 10. Effect of rigidity ratio r on the response to nonstationary excitation.
—— : Theory ····· : Simulation

Fokker-Planck equation approach which is based on the expression of polylinear hysteretic characteristics in the form of the first-order quasi-linear differential equations by introducing an extra state variable for each elementary elasto-plastic component. It is emphasized that the method is applicable to the nonstationary stochastic response

analysis of hysteretic systems which have strongly nonlinear characteristics accompanied by the fluctuation of the center of hysteresis.

Numerical examples of a bilinear hysteretic system to both stationary and nonstationary Gaussian white noise excitations have been presented. The results of the present analytical method compared satisfactorily with the results of the Monte Carlo simulation. In particular, for the case of strong nonlinearity with a low rigidity ratio and a high excitation level the present method gives much more accurate results as compared with the other methods including statistical linearization techniques.

References

1) Caughey, T.: Derivation and Application of the Fokker-Planck Equation to Discrete Nonlinear Dynamic Systems Subjected to White Random Excitation, J. Acoust. Soc. Amer., Vol. 35, No. 11, 1963, pp. 1683–1692.
2) Caughey, T.: Equivalent Linearization Techniques, J. Acoust. Soc. Amer., Vol. 35, No. 11, 1963, pp. 1706–1711.
3) Lutes, L.D.: Approximate Technique for Treating Random Vibration of Hysteretic Systems, J. Acoust. Soc. Amer., Vol. 48, No. 1, 1970, pp. 299–306.
4) Kobori, T., R. Minai and Y. Suzuki: Statistical Linearization Techniques of Hysteretic Structures to Earthquake Excitations, Bull. Disas. Prev. Res. Inst., Kyoto Univ., Vol. 23, Part 3–4, No. 215, 1973, pp. 111–135.
5) Kaul, M.K. and J. Penzien: Stochastic Seismic Analysis of Yielding Offshore Towers, Proc. ASCE, Vol. 100, No. EM5, 1974, pp. 1025–1038.
6) Kobori, T., R. Minai and Y. Suzuki: Nonstationary Random Response of Bilinear Hysteretic Systems, Theoretical and Applied Mechanics, Vol. 24, 1974, pp. 143–152.
7) Lutes, L.S. and H. Takemiya: Random Vibration of a Yielding Oscillator, Proc. ASCE, Vol. 100, No. EM2, 1974, pp. 343–358.
8) Iwan, W.D.: The Distributed-Element Concept of Hysteretic Modeling and Its Application to Transient Response Problems, Proc. of the Fourth World Conf. on Earthquake Engineering, Santiago, Chile, 1969, A4, pp. 45–57.
9) Kuznetsov, P. I., R. L. Stratonovich and V.I. Tikhonov: Quasi-moment Functions in the Theory of Random Processes, Theory Prob. Applications, Vol. 5, No. 2, 1960, pp. 80–97.
10) Saragoni, G.R. and G.C. Hart: Simulation of Artificial Earthquakes, Int. J. Earthq. Engrg Struct. Dyn., Vol. 2, No. 3, 1974, pp. 249–267.
11) Jennings, P.C. and R. Husid: Collapse of Yielding Structures During Earthquakes, Proc. ASCE, Vol. 94, No. EM5, 1968, pp. 1045–1065.